

X-ray Structure of Human Acid- β -Glucosidase Covalently Bound to Conduritol-B-Epoxyde

IMPLICATIONS FOR GAUCHER DISEASE*[§]◆

Received for publication, March 14, 2005, and in revised form, April 4, 2005
Published, JBC Papers in Press, April 6, 2005, DOI 10.1074/jbc.M502799200

Lakshmanane Premkumar^{‡§}, Anu R. Sawkar[¶], Svetlana Boldin-Adamsky[§], Lilly Toker^{||},
Israel Silman^{||}, Jeffery W. Kelly^{¶*}, Anthony H. Futerman^{‡‡}, and Joel L. Sussman^{‡§§}

From the [‡]Departments of Structural Biology, ^{||}Neurobiology, and [§]Biological Chemistry, Weizmann Institute of Science, Rehovot 76100, Israel, and the [¶]Department of Chemistry and The Skaggs Institute for Chemical Biology, The Scripps Research Institute, La Jolla, California 92037

Gaucher disease is an inherited metabolic disorder caused by mutations in the lysosomal enzyme acid- β -glucosidase (GlcCerase). We recently determined the x-ray structure of GlcCerase to 2.0 Å resolution (Dvir, H., Harel, M., McCarthy, A. A., Toker, L., Silman, I., Futerman, A. H., and Sussman, J. L. (2003) *EMBO Rep.* 4, 704–709) and have now solved the structure of GlcCerase conjugated with an irreversible inhibitor, conduritol-B-epoxyde (CBE). The crystal structure reveals that binding of CBE to the active site does not induce a global conformational change in GlcCerase and confirms that Glu³⁴⁰ is the catalytic nucleophile. However, only one of two alternative conformations of a pair of flexible loops (residues 345–349 and 394–399) located at the entrance to the active site in native GlcCerase is observed in the GlcCerase-CBE structure, a conformation in which the active site is accessible to CBE. Analysis of the dynamics of these two alternative conformations suggests that the two loops act as a lid at the entrance to the active site. This possibility is supported by a cluster of mutations in loop 394–399 that cause Gaucher disease by reducing catalytic activity. Moreover, *in silico* mutational analysis demonstrates that all these mutations stabilize the conformation that limits access to the active site, thus providing a mechanistic explanation of how mutations in this loop result in Gaucher disease.

Gaucher disease, the most common lysosomal storage disorder (1), is caused by mutations in the gene encoding acid- β -glucosidase (GlcCerase),¹ which result in intracellular accumulation of the lipid substrate, glucosylceramide (2, 3). These mutations diminish GlcCerase activity either by reducing enzyme activity or by reducing the lysosomal enzyme concentration. Enzyme activity is reduced in mutations that affect the turnover number, substrate affinity, or activator binding (4). Lysosomal enzyme concentration is reduced by mutations that compromise folding in the endoplasmic reticulum, resulting in proteasomal degradation of the protein (5).

We recently solved the three-dimensional structure of recombinant GlcCerase (Cerezyme®), the enzyme used in enzyme replacement therapy in Gaucher disease (6). The structure comprises three non-contiguous domains, with the catalytic site located in domain III (residues 76–381 and 416–430), a (β/α)₈ (TIM) barrel. The function of the two non-catalytic domains is not known, but mutations that cause Gaucher disease are found in all three domains.

To determine whether substrate or inhibitor binding can induce conformational change(s) in GlcCerase, and to try to gain insight into possible roles of the non-catalytic domains, we have now determined the crystal structure of a conjugate of GlcCerase with an irreversible inhibitor, conduritol-B-epoxyde (1,2-anhydro-*myo*-inositol; CBE) (7). Binding of CBE did not induce a global conformational change in the structure of GlcCerase but permitted us to assign a role to two surface loops found at the entrance to the active site and to suggest how mutations in one of these loops might reduce catalytic activity, thus leading to Gaucher disease.

EXPERIMENTAL PROCEDURES

Materials—Cerezyme® was obtained from patient leftovers. CBE was from Biomol (Plymouth, PA), and *N*-glycosidase F was from Roche Applied Science (Mannheim, Germany). *N*-(6-(7-nitrobenzo-2-oxa-1,3-diazol-4-yl)amino)hexanoyl-D-erythro-glucosylsphingosine (C₆-NBD-GlcCer) was prepared as described (8).

Crystallization and Data Collection—Cerezyme® was crystallized after partial deglycosylation using *N*-glycosidase F (6), which is capable of cleaving all types of asparagine bound *N*-glycans (9, 10), but did not produce complete deglycosylation of native Cerezyme® under the experimental conditions employed (6). GlcCerase-CBE crystals were obtained by soaking native GlcCerase crystals overnight at 19 °C in mother liquor (1 M (NH₄)₂SO₄, 170 mM guanidinium HCl, 20 mM KCl, 100 mM acetate, pH 4.6) containing 1 mM CBE. The crystals were cryoprotected with a gradient of 5–25% glycerol. Data were collected

* This work was supported by the National Gaucher Foundation, European Community 5th Framework Contract QL2-CT-2002-00988 (SPINE), an Israel Ministry of Science and Technology grant to the Israel Structural Proteomics Center, the Kimmelman Center for Biomolecular Structure and Assembly, the Benozio Center for Neurosciences, the Skaggs Institute for Chemical Biology, and a National Science Foundation Predoctoral Fellowship (to A. R. S.). The costs of publication of this article were defrayed in part by the payment of page charges. This article must therefore be hereby marked "advertisement" in accordance with 18 U.S.C. Section 1734 solely to indicate this fact.

◆ This article was selected as a Paper of the Week.

[§] The on-line version of this article (available at <http://www.jbc.org>) contains supplemental Figs. 1 and 2 (both figures contain movies).

The atomic coordinates and structure factors (code 1Y7V) have been deposited in the Protein Data Bank, Research Collaboratory for Structural Bioinformatics, Rutgers University, New Brunswick, NJ (<http://www.rcsb.org/>).

** Is the Lita Annenberg Hazen Professor of Chemistry at the Scripps Research Institute.

^{‡‡} Is the Joseph Meyerhoff Professor of Biochemistry at the Weizmann Institute of Science. To whom correspondence should be addressed: Dept. of Biological Chemistry, Weizmann Inst. of Science, Rehovot 76100, Israel. Tel.: 972-8-9342704; Fax: 972-8-9344112; E-mail: tony.futerman@weizmann.ac.il.

^{§§} Is the Morton and Gladys Pickman Professor of Structural Biology in the Weizmann Institute of Science.

¹ The abbreviations used are: GlcCerase, acid- β -glucosidase; CBE, conduritol-B-epoxyde; C₆-NBD-GlcCer, *N*-(6-(7-nitrobenzo-2-oxa-1,3-diazol-4-yl)amino)hexanoyl-D-erythro-glucosylsphingosine; MES, 4-morpholinoethanesulfonic acid.

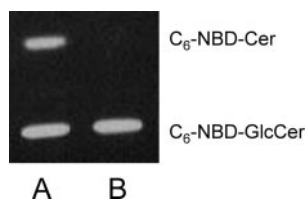


FIG. 1. **Effect of CBE on GlcCerase activity.** GlcCerase crystals (~ 0.5 – $1 \mu\text{g}$ of protein), into which CBE had (B) or had not been (A) soaked were redissolved in the GlcCerase reaction buffer and assayed for GlcCerase activity using C_6 -NBD-GlcCer as substrate. Levels of activity were determined by analysis of formation of C_6 -NBD-ceramide (C_6 -NBD-Cer).

TABLE I
Data collection statistics

Data for the outer shell are in parentheses.	
R-AXIS IV ⁺⁺	
Wavelength (Å)	1.5418
Space group	C222 ₁
Unit cell (Å)	$a = 104.49$ $b = 285.61$ $c = 91.51$
Resolution range (Å)	30–2.4
Unique reflections	53,193
Completeness (%)	97.0 (95.7)
$\langle I \rangle / \sigma(I)$	12.75 (4.88)
R_{meas} (%)	8.8 (30.0)

“in-house” at 100 K on an R-AXIS IV⁺⁺ imaging plate system mounted on an RU300 x-ray generator operating at 50 kV and 90 mA. Data were processed using XDS and XSCALE (11). Reflections were converted using XDSCONV to a format suitable for CNS, and a list of randomly generated test reflections was inherited from a master list for the native orthorhombic crystal form of GlcCerase (6). Table I summarizes data collection and processing.

Structure Determination and Refinement—The GlcCerase-CBE structure was solved using the difference Fourier technique, exploiting the native isomorphous crystal structure of GlcCerase (Protein Data Bank ID code 1OGS). The 1OGS coordinates were used as a starting model for rigid body refinement (30–2.4 Å resolution) in CNS (12). After a round of simulated annealing, $F_o - F_c$ and $2F_o - F_c$ maps were used to fit the CBE molecule, two carbohydrate moieties, and 10 sulfate molecules. XtalView (13) was used for all model building and repositioning of atoms in the model structure. The chemical model of cyclohexitol was built using CS Chem3D Pro (version 5.0), and energy minimization was performed on the inhibitor model using the molecular dynamics utilities of CS Chem3D Pro (www.camsoft.com). These models were used to generate suitable topology and parameter files for CNS using the PRODRG2 server (14) prior to map fitting. 2-Fold non-crystallographic symmetry restraints were applied in all the refinement cycles. As the map phases improved with subsequent simulated annealing and individual B-refinements, additional water molecules were added. The model was further refined by positional maximum likelihood minimization and by individual B-factor refinement. The results are summarized in Table II. Figs. 2, 5, and 6 were generated using PyMOL (www.pymol.org). Side chain modeling for the *in silico* mutational analysis was performed using program O (15), Swiss PDB Viewer (16), and the Swiss PDB server (www.swissmodel.expasy.org).

Activity Measurements—GlcCerase activity was assayed using 7.5 μM C_6 -NBD-GlcCer in 50 mM MES, pH 5.5, as described for other short acyl chain GlcCer derivatives (8).

RESULTS

Structure of the GlcCerase-CBE Complex—Initial experiments were performed to determine whether CBE was able to bind to GlcCerase crystals. Upon redissolving in the GlcCerase reaction buffer, GlcCerase crystals were fully active, but crystals into which CBE had been soaked were devoid of catalytic activity (Fig. 1).

X-ray data for the GlcCerase-CBE complex were collected (Table I) and refined to 2.4 Å resolution (Table II). From the initial $F_o - F_c$ and the $2F_o - F_c$ maps, it is apparent that CBE binds only to Glu³⁴⁰ (Fig. 2) and not to any other residues, including Asp⁴⁴³ and Asp⁴⁴⁵ (17). The proposed reaction mech-

TABLE II
Refinement and model statistics

Resolution range (Å)	30–2.4
R_{work} (%) ^a	23.94
R_{free} (%) ^b	27.95
Average B-factor (Å ²)	36.86
Root mean square deviations from ideal values:	
Bond lengths (Å)	0.012
Bond angles (°)	1.655
Torsion angles (°)	24.39
Improper torsion angles (°)	1.10
Estimated coordinate error:	
Low resolution cut-off (Å)	5.0
ESD from Luzzati plot (Å) ^c	0.37
ESD from SIGMAA (Å) ^c	0.66
Ramachandran outliers (%)	0.4
Number of protein atoms	7860
Number of hetero atoms	429

^a $R_{\text{work}} = \frac{\sum ||F_o| - |F_c||}{\sum |F_o|}$, where F_o denotes the observed structure factor amplitude and F_c the structure factor amplitude calculated from the model.

^b R_{free} is for 5% of randomly chosen reflections excluded from the refinement.

^c ESD, estimated standard deviation.

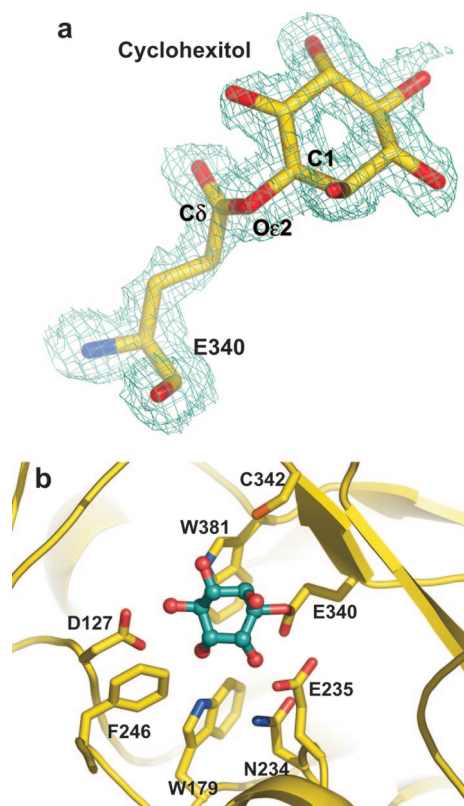


FIG. 2. **Binding of CBE to the GlcCerase active site.** *a*, $F_o - F_c$ difference omit map (contoured to 3.2σ level) of the cyclohexitol ring and of Glu³⁴⁰ in the active site of GlcCerase. *b*, active site of GlcCerase with bound cyclohexitol. The cyclohexitol ring is in cyan, and its hydroxyl groups are in red. The catalytic nucleophile (Glu³⁴⁰ (E340)), the proposed acid/base catalyst (Glu²³⁵ (E235)), and the residues in proximity to CBE are displayed in CPK colors.

anism (7) involves protonation of the epoxide oxygen of CBE by the catalytic acid/base, followed by nucleophilic attack at C1 of the cyclohexitol ring, causing diaxial opening of the epoxide and formation of a nucleophile-cyclohexitol ester bond (Fig. 3). The crystal structure supports this mechanism, since the distance between C1 of the cyclohexitol and Glu³⁴⁰Oε2 is 1.43 Å, confirming Glu³⁴⁰ as the active-site nucleophile (Fig. 2). Moreover, the distance between the epoxide oxygen of CBE, oriented similarly to the cyclohexitol ring, and Glu²³⁵Oε, is within hy-

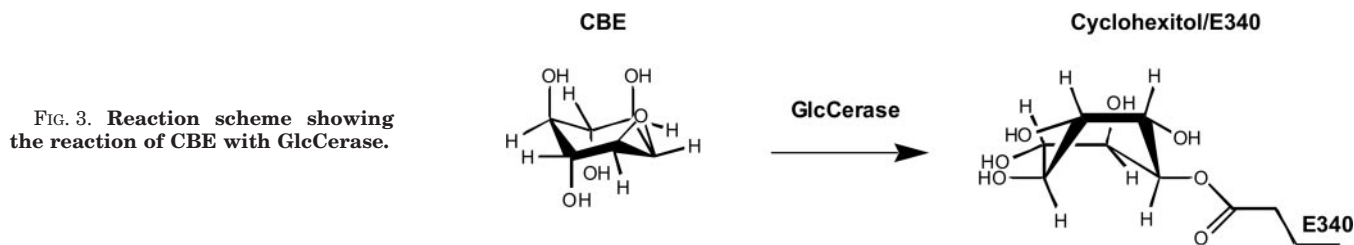


FIG. 3. Reaction scheme showing the reaction of CBE with GlcCerase.

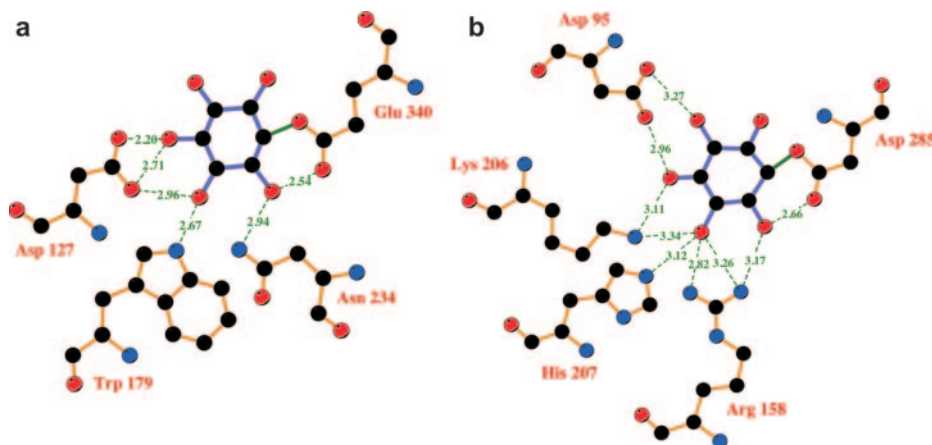


FIG. 4. Comparison of the interaction of CBE with GlcCerase and with a plant β -D-glucan glucohydrolase. Hydrogen bonding interactions of the cyclohexitol ring in the active sites of GlcCerase (a) and a plant β -D-glucan glucohydrolase (b) are shown, with green dashed lines indicating hydrogen bonds (lengths in Å) and with the intact green line representing the covalent bond between C1 of the cyclohexitol and the catalytic nucleophiles of the enzymes. The figure was prepared using Ligplot 4.2 (28).

drogen-bonding distance, consistent with the role of Glu²³⁵ as the acid/base catalyst (18) (Fig. 2b).

Additional residues in proximity to the cyclohexitol in GlcCerase (Fig. 4a) were compared with those found in a plant β -D-glucan glucohydrolase (19) (Fig. 4b), a member of the same glucohydrolase family. In contrast to the chair conformation adopted by the cyclohexitol upon binding to a plant β -D-glucan glucohydrolase (19), the cyclohexitol is found in a boat conformation in GlcCerase, with hydrogen bonds to Asn²³⁴O δ 1 and N δ 2, Glu³⁴⁰O ϵ 1, Trp¹⁷⁹N ϵ 1, and Asp¹²⁷O δ 1 and O δ 2 (Fig. 4a). The boat conformation is stabilized by tight hydrogen-bonding interactions between C4-OH of the cyclohexitol and Asp¹²⁷ and between C3-OH and Asp¹²⁷ and Trp¹⁷⁹.

Characterization of a Lid at the Entrance to the Active Site—Superimposition of the native GlcCerase structure on that of GlcCerase-CBE revealed a root mean square deviation of only \sim 0.32 Å, demonstrating that GlcCerase does not undergo a global structural change upon binding CBE. However, examination of the root mean square deviations of individual residues revealed a significant difference between native GlcCerase and GlcCerase-CBE with respect to the conformation of two loops, Ser³⁴⁵–Glu³⁴⁹ (loop 1) and Val³⁹⁴–Asp³⁹⁹ (loop 2). In native GlcCerase, the two molecules in the asymmetric unit display two alternative conformations (6) for both of these loops (Fig. 5a). In loop 2, a major conformational difference is seen in the positions of Asn³⁹⁶ and Phe³⁹⁷ in the two asymmetric units (Fig. 5c), and in loop 1 a more modest difference is seen in the conformations of Lys³⁴⁶ and Glu³⁴⁹ (Fig. 5b). In contrast, the two molecules in the asymmetric unit of the GlcCerase-CBE crystals adopt only one of these two conformations.

Interestingly, the two loops are located on the surface of GlcCerase at the entrance to the active site. In the conformation adopted in the GlcCerase-CBE structure, Asn³⁹⁶ and Phe³⁹⁷ are positioned such that access to the active site is not restricted (Fig. 6a). However, in the other alternative conformation, which is displayed only in the native GlcCerase structure, the side chains of Asn³⁹⁶ and Phe³⁹⁷ swing over and block the entrance to the active site (Fig. 6b), suggesting that this

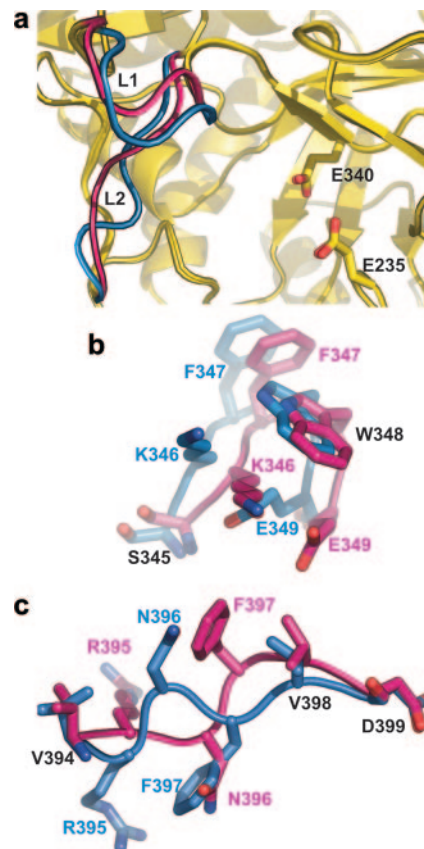


FIG. 5. Alternative conformations of loops 1 and 2 in GlcCerase. a, the alternative conformations of the two loops, L1 (Ser³⁴⁵–Glu³⁴⁹) and L2 (Val³⁹⁴–Asp³⁹⁹) found in the two asymmetric units of native GlcCerase are indicated in pink and marine, corresponding to the closed and open conformations, respectively. b and c, conformational changes in individual residues in loops 1 (b) and 2 (c), color-coded as in a, with residues indicated in each loop.

loop serves as a lid regulating access to the active site in GlcCerase. Thus, these two loops allow GlcCerase to exist in either an open (Fig. 6a) or closed (Fig. 6b) conformation, depending on the orientation of the loops. The movies in supplemental Figs. 1 and 2 illustrate the dynamics of the movement of these two loops (29).

Analysis of the distribution of mutant forms of GlcCerase that cause Gaucher disease reveals a cluster of mutations in

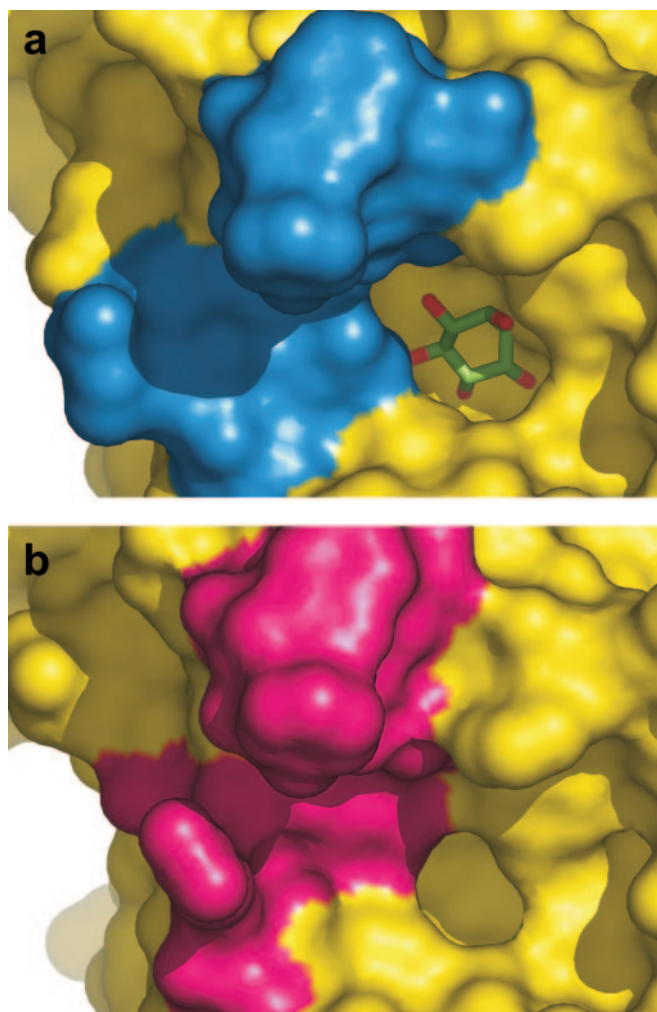


FIG. 6. Surface of GlcCerase illustrating the open and closed conformations. *a*, the open conformation in which CBE is bound to the active site. *b*, the closed conformation in which the surface lid restricts access to the active site. Color coding is the same as described for Fig. 5.

loop 2, including V394L (2), R395P (20), N396T (21), V398L/F (22, 23), and D399N (24). *In silico* analysis of these mutants is consistent with either destabilization of the open conformation or stabilization of the closed conformation (Table III), thus limiting substrate access to the active site. For instance, V394L, one of the six most common mutations in Gaucher disease (2), results in enhanced hydrophobic interactions of Leu³⁹⁴ with Trp³⁹³ and Phe²⁴⁶ in the closed conformation; conversely, this same mutation destabilizes the open conformation, since the larger side chain cannot interact with the aromatic side chains of Trp³⁹³ and Phe²⁴⁶. Likewise, R395P destabilizes the open conformation due to the loss of a stabilizing salt bridge with Glu³⁸⁸. N396T results in additional hydrogen bonding between Thr³⁹⁶ and the carbonyl oxygens of residues Glu³⁸⁸ and Gly³⁸⁹ in the closed conformation but in reduced H-bonding with Asp¹²⁷ in the open conformation. Thus, the structure of GlcCerase complexed to CBE gives insight into the mechanism by which catalytic activity is reduced by mutations in this newly identified lid that controls access to the active site.

DISCUSSION

In the current study we have solved the x-ray structure of GlcCerase covalently bound to CBE. Using this structure, we confirmed earlier assignments, based on electrospray tandem mass spectrometry, that Glu³⁴⁰ is the nucleophile and Glu²³⁵ is the acid/base catalyst (25). Since catalytic activity was completely inhibited by binding of the cyclohexitol to Glu³⁴⁰, and since we saw no binding to any other residues, we can also exclude the possibility that the inhibitory effect of CBE on GlcCerase activity is due to binding to Asp⁴⁴³ and Asp⁴⁴⁵, as proposed earlier (17).

There are no global structural changes between the GlcCerase-CBE structure and that of native GlcCerase, suggesting that binding of inhibitors to the active site, and presumably also binding of the lipid substrate, does not induce a major conformational change. This also serves as proof of concept that the GlcCerase structure can be used as a starting point for designing structure-based drugs aimed at restoring the activity of defective GlcCerase (3). Important among these are the small molecular weight chaperones that, upon binding to the active site, restore trafficking of improperly folded GlcCerase out of the endoplasmic reticulum and through the secretory pathway to lysosomes, thereby restoring normal, or near-normal, lysosomal GlcCerase levels (5, 26).

Although there are no global structural changes, we did detect a significant structural change in two surface loops at the entrance to the active site that appear to act as a lid controlling access to the active site. Interestingly, a lid has also been detected in a number of glycosyltransferases (27). In the glycosyltransferases, one or two flexible loops near the sub-

TABLE III
In silico mutational analysis of loop Val³⁹⁴-Asp³⁹⁹

Non-bonded contacts, salt bridges, and hydrogen bonds are listed for the closed and open conformations for wild-type GlcCerase and for the mutants.

Mutation	Closed conformation	Open conformation
V394L	Contacts with Phe ²⁴⁶ and Trp ³⁹³	Contacts with Phe ²⁴⁶ and Trp ³⁹³
R395P	Contacts with Pro ²⁴⁵ , Phe ²⁴⁶ , Arg ³⁹⁵ , and Trp ³⁹³	Contact with Pro ²⁴⁵
N396T	No interaction	Salt bridge to Glu ³⁸⁸
V398L	No interaction	No interaction
V398F	No H-bond	H-bond to Asp ¹²⁷
D399N	H-bonds to Glu ³⁸⁸ (O) and Gly ³⁸⁹ (O)	H-bond to Asp ¹²⁷
	Contacts with Phe ¹²⁸ and Phe ³⁹⁷	Contact with Phe ¹²⁸
	Contact with Phe ³⁹⁷	No interaction
	Contacts with Phe ¹²⁸ and Phe ³⁹⁷	Contact with Phe ¹²⁸
	Contact with Phe ³⁹⁷	No interaction
	Salt bridge to Arg ³⁵⁹ and H-bonds to Gln ⁴¹⁴ (N), Arg ³⁵³ (O), and Ser ⁴⁰⁰ (N)	Salt bridge to Arg ³⁵⁹
	H-bonds to Met ⁴¹⁶ (S δ), Val ³⁴³ (O), and Ser ⁴⁰⁰ (N)	H-bond to Gln ⁴¹⁴ (N), Ser ⁴⁰⁰ (N), and Arg ³⁵³ (N)
		H-bonds to Ser ⁴⁰⁰ (N) and Gln ⁴¹⁴

strate binding site undergo a marked conformational change from an open to a closed conformation upon binding the donor substrate. The flexibility of these loops is crucial for the catalytic activity of the glycosyltransferases (27).

In GlcCerase, the role of one of the two surface loops in governing access to the active site is supported by the reduced affinity of GlcCerase for CBE in various GlcCerase mutations, such as V394L (4), R395P, and N396T (20), although V394L also displays reduced thermostability and reduced stability at low pH (4), implying a disruption of structural integrity that may result in rapid lysosomal degradation. Thus, loop mutations may both decrease the catalytic activity of GlcCerase and reduce its lysosomal enzyme concentration. Unfortunately, sufficient amounts of GlcCerase mutated in residues in these loops are not available for crystallization studies, but *in silico* mutational analysis is entirely consistent with the lid being in the closed conformation in the mutated proteins, which would prevent access of GlcCer to the active site. The discovery of a lid regulating access to the GlcCerase active site provides the first mechanistic insight into how GlcCerase mutations result in reduced catalytic activity and as a consequence cause Gaucher disease.

REFERENCES

1. Futerman, A. H., and van Meer, G. (2004) *Nat. Rev. Mol. Cell. Biol.* **5**, 554–565
2. Beutler, E., and Grabowski, G. A. (2001) in *The Metabolic and Molecular Bases of Inherited Disease* (Scriver, C. R., Sly, W. S., Childs, B., Beaudet, A. L., Valle, D., Kinzler, K. W., and Vogelstein, B., eds) 8th Ed., pp. 3635–3668, McGraw-Hill Inc., New York
3. Futerman, A. H., Sussman, J. L., Horowitz, M., Silman, I., and Zimran, A. (2004) *Trends Pharmacol. Sci.* **25**, 147–151
4. Grace, M. E., Newman, K. M., Scheinker, V., Berg-Fussman, A., and Grabowski, G. A. (1994) *J. Biol. Chem.* **269**, 2283–2291
5. Sawkar, A. R., Cheng, W. C., Beutler, E., Wong, C. H., Balch, W. E., and Kelly, J. W. (2002) *Proc. Natl. Acad. Sci. (U. S. A.)* **99**, 15428–15433
6. Dvir, H., Harel, M., McCarthy, A. A., Toker, L., Silman, I., Futerman, A. H., and Sussman, J. L. (2003) *EMBO Rep.* **4**, 704–709
7. Legler, G. (1990) *Adv. Carbohydr. Chem. Biochem.* **48**, 319–384
8. Meivar-Levy, I., Horowitz, M., and Futerman, A. H. (1994) *Biochem. J.* **303**, 377–382
9. Tarentino, A. L., Gomez, C. M., and Plummer, T. H., Jr. (1985) *Biochemistry* **24**, 4665–4671
10. Chu, F. K. (1986) *J. Biol. Chem.* **261**, 172–177
11. Kabsch, W. (1993) *J. Appl. Crystallogr.* **26**, 795–800
12. Brunger, A. T., Adams, P. D., Clore, G. M., DeLano, W. L., Gros, P., Grosse-Kunstleve, R. W., Jiang, J. S., Kuszewski, J., Nilges, M., Pannu, N. S., Read, R. J., Rice, L. M., Simonson, T., and Warren, G. L. (1998) *Acta Crystallogr. Sect. D Biol. Crystallogr.* **54**, 905–921
13. McRee, D. E. (1999) *J. Struct. Biol.* **125**, 156–165
14. Schuttelkopf, A. W., and van Aalten, D. M. (2004) *Acta Crystallogr. Sect. D Biol. Crystallogr.* **60**, 1355–1363
15. Jones, T. A. (1978) *J. Appl. Crystallogr.* **11**, 268–272
16. Guex, N., and Peitsch, M. C. (1997) *Electrophoresis* **18**, 2714–2723
17. Dinur, T., Osiecki, K. M., Legler, G., Gatt, S., Desnick, R. J., and Grabowski, G. A. (1986) *Proc. Natl. Acad. Sci. (U. S. A.)* **83**, 1660–1664
18. Henrissat, B., Callebaut, I., Fabrega, S., Lehn, P., Mornon, J. P., and Davies, G. (1995) *Proc. Natl. Acad. Sci. (U. S. A.)* **92**, 7090–7094
19. Hrmova, M., Varghese, J. N., De Gori, R., Smith, B. J., Driguez, H., and Fincher, G. B. (2001) *Structure (Camb.)* **9**, 1005–1016
20. Amaral, O., Marcao, A., Sa Miranda, M., Desnick, R. J., and Grace, M. E. (2000) *Eur. J. Hum. Genet.* **8**, 95–102
21. Amaral, O., Pinto, E., Fortuna, M., Lacerda, L., and Sa Miranda, M. C. (1996) *Hum. Mutat.* **8**, 280–281
22. Seeman, P. J., Finckh, U., Hoppner, J., Lakner, V., Liebisch, I., Grau, G., and Rolfs, A. (1996) *Neurology* **46**, 1102–1107
23. Stone, D. L., van Diggelen, O. P., de Klerk, J. B., Gaillard, J. L., Niermeijer, M. F., Willemsen, R., Tayebi, N., and Sidransky, E. (1999) *Eur. J. Hum. Genet.* **7**, 505–509
24. Beutler, E., and Gelbart, T. (1994) *Hum. Genet.* **93**, 209–210
25. Miao, S., McCarter, J. D., Grace, M. E., Grabowski, G. A., Aebbersold, R., and Withers, S. G. (1994) *J. Biol. Chem.* **269**, 10975–10978
26. Fan, J. Q. (2003) *Trends Pharmacol. Sci.* **24**, 355–360
27. Qasba, P. K., Ramakrishnan, B., and Boeggeman, E. (2005) *Trends Biochem. Sci.* **30**, 53–62
28. Wallace, A. C., Laskowski, R. A., and Thornton, J. M. (1995) *Protein Eng.* **8**, 127–134
29. Zeev-Ben-Mordehai, T., Silman, I., and Sussman, J. L. (2003) *Biopolymers* **68**, 395–406